Wind-Driven Currents on the West Florida Shelf

GARY T. MITCHUM AND W. STURGES

Department of Oceanography, Florida State University, Tallahassee 32306

(Manuscript received 7 October 1981, in final form 24 June 1982)

ABSTRACT

Three weeks of current-meter, wind and sea-level data off Cedar Key, Florida are analyzed. Currents and sea level are found to be coherent with alongshore wind stress in the "synoptic" band (~0.05–0.25 cycle per day) and to lag it by approximately half a day. Little coherence is found with cross-shelf wind stress.

At the inshore mooring (22 m depth) currents are nearly barotropic for these winter 1978 data. A linear parameterization of bottom stress in the barotropic alongshore current leads to a bottom friction parameter r of 0.01–0.02 cm s^{-1} using coastal wind stress. No significant steady alongshore slope is found during this short interval. The dominant momentum balance in the alongshore direction is between wind and bottom stress. The offshore frictional length scale (Csanady, 1978) is estimated to be 75–100 km, which implies a seaward extent to a depth of about 30 m.

At the offshore mooring (44 m depth) there is vertical shear between the currents at 9 and 39 m. The upper cross-shelf component, which is large relative to that at the inshore mooring, is consistent with Ekman transport while the lower record shows a return flow. The u, v velocity components correlate significantly at the offshore mooring and lead to an upper layer $\overline{uv}$ gradient on the order of 10^{-5} cm^2 s^{-2} between the arrays (75 km separation).

The sea-level fluctuations are consistent with a geostrophic balance in the cross-shelf momentum equation with a length scale of 170 km (approximately equal to the shelf width).

1. Introduction

In recent years, the importance of bottom friction to low-frequency circulation in shallow water has been realized and a "coastal boundary layer" theory developed. Csanady (1976), considering low-frequency motions superimposed on higher frequency background currents, showed that the quadratic bottom-friction law may be parameterized as being linear in the near-bottom velocity with the proportionality constant (denoted r) being dependent upon the amplitude of the high-frequency motions. This coefficient can be determined from simultaneous observations of currents and wind stress in the manner of Scott and Csanady (1976). Objections have been raised by Beardsley and Winant (1979) concerning the method used by Scott and Csanady but, in principle at least, the r value can be estimated from data and the depth-integrated alongshore momentum equation.

Observational studies on the West Florida shelf were carried out during the years 1973–75 (Koblinsky and Niiler, 1980) off Tampa; however, the arrays were concentrated near the shelf break. Using those data, Niiler (1976) studied the Loop Current influence on the shelf currents but found no coherence with wind stress except at the shallowest mooring in 105 m of water. Even there the phase seemed hard to explain as the currents seemed to either *lead* stress by about 3 days or lag it by 7 days at periods of around 10 days. Koblinsky (1979) also used the data to study the tidal motions on the West Florida Shelf.

A study of relationships between wind and sea level (Cragg *et al.*, 1982; see also Cragg and Sturges, 1974) in this area implied the existence of broad alongshore geostrophic flows driven by the wind. This conclusion, that there is geostrophic balance in the cross-shelf momentum equation with the length scale coinciding with the distance to the shelf break, is a widely accepted notion; some support for this idea has been presented from observations off Oregon (e.g., Huyer *et al.*, 1978; Allen and Kundu, 1978). On the east coast, much important work on the coastal boundary layer has been done off Long Island (Scott and Csanady, 1976; Han and Mayer, 1981; Pettigrew, 1981). The data we now address are approximately 23 days of current-meter observations made during February and March of 1978. Two instruments were deployed near the 45 m isobath and two near the 25 m isobath on the West Florida Shelf off Cedar Key, Florida (Fig. 1).

2. Data

During the late winter the water column was nearly unstratified. From historical data (SUSIO,[1] 1975) and

[1] State University System Institute of Oceanography, St. Petersburg, FL.

0022-3670/82/111310-08$06.00

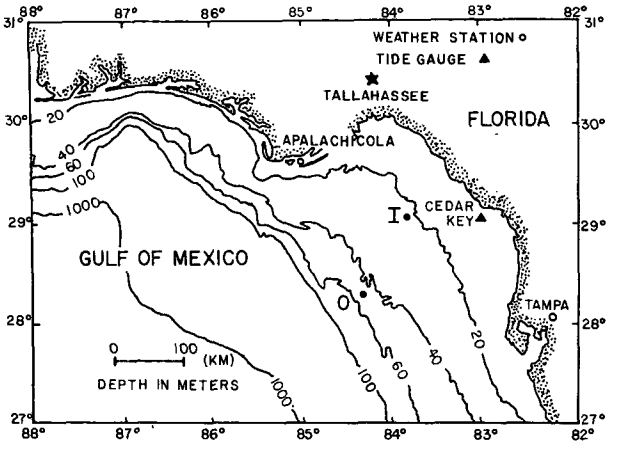

FIG. 1. Map of the study area showing the tide gauge (triangle) and weather stations (open circles) used. The current-meter arrays (closed circles) are labeled I (inshore) and O (offshore).

some limited hydrographic data obtained while placing the arrays, the Brunt-Väisälä frequency was estimated to be $\sim 10^{-3}$ Hz. The bottom in this area is chiefly sand and sandy mud (Chesser, 1974). The water is usually clear, and small-leaved plants grow on the bottom. The Loop Current during this time period was never found north of 27.5°N (Steven Baig, National Environmental Satellite Service, private communication) and was generally much farther to the south. Its effect on the shelf currents is therefore considered small, and is not considered here. All current meters used were Aanderaa units. The moorings used sub-surface flotation and are described in Table 1. The time series for the current meters were rotated parallel to the local isobaths such that the v component is along 31°W of north inshore and 39°W of north offshore. The series were filtered (see Table 2) and subsampled to avoid aliasing. These series were later used in cross-spectral analyses with sea-level and wind-stress series. The effects of this filtering were removed when computing the spectra.

TABLE 1. Description of the moorings deployed from 2/24/78 to 3/20/78 off Cedar Key, Florida. The Aanderaa current meters used average rotor counts for the sampling interval shown and sample the direction at the end of the interval. The depths shown are the meter depth/water depth. For example, 12/22 means the current meter was at a depth of 12 m and the water depth was 22 m.

Mooring	Mooring location	Distance offshore (km)	Sampling interval (min)	Meter	Depths (m)
I	29°05'N 83°50'W	75	5	1	12/22
				2	17/22
O	28°18'N 84°20'W	150	10	1	9/44
				2	39/44

TABLE 2. Distribution of variance in the data series. The wind stress components and sea level are 3 h and 1 h data, respectively, and have not been filtered. The original current-meter records were filtered with a Gaussian filter of standard deviation 2 h and subsampled at 1 h intervals. Means and linear trends listed were removed before spectral analysis and the total variance listed is after also tapering 10% on each end with a split cosine bell taper. The time period is 2200 2/24/78 to 1600 3/19/78. The numbers given for the synoptic band and the tidal components are percents of the total variance. All units are cgs and spectra are recolored for filter effects.

	Mean	Linear trend	Total variance	Synoptic band	Tidal components
Sea level	1.37	−0.0073	1115	12.7	63.1
τ^y	−0.0298	−0.00054	0.0515	71.0	—
τ^x	0.0101	−0.00025	0.0101	43.0	—
V-O1	−0.95	−0.046	211.6	61.8	9.4
U-O1	1.26	−0.014	276.7	21.9	49.1
V-O2	2.20	−0.030	75.8	71.5	6.6
U-O2	1.15	−0.0052	119.9	9.0	69.2
V-I1	−0.66	−0.033	162.9	78.1	7.9
U-I1	−1.56	0.0022	283.6	1.9	81.1
V-I2	−0.66	−0.031	177.2	78.3	9.6
U-I2	−1.68	0.0011	267.6	1.8	80.3

Our primary interest in this study was the current variability associated with synoptic-scale meteorological forcing which has periods of approximately 2 days to a week. To isolate this band, the series were low-passed and then linearly detrended to remove variability on time scales greater than the record length (~23 days). This frequency band is referred to here as the "synoptic" band and the detrended, low-passed series are shown in Fig. 2.

The Aanderaa current meters used in this experiment tend to have rotor overspin in strong wave motions (Beardsley *et al.*, 1977). Koblinsky and Niiler (1980) compared Aanderaa meters to adjacent VACM records on the West Florida Shelf and found good results (their Figure 2). We plotted the ratio, v/τ vs τ, where v is current speed and τ wind-stress magnitude, to look for any trend at the higher stress values that might indicate overspin. No such trend is seen (Fig. 3). Our records were taken during a time when there were no severe storms and, consequently, relatively small surface waves. Thus the quality of the current-meter records appears to be very good.

A more serious possible drawback to the current-meter data is the brevity of the record. The 23-day record length includes only three or four synoptic events. The length of the record was dictated by ship schedules and by a desire to avoid long untended moorings on account of heavy commercial fishing in the study area. (In fact, a set of moorings placed later in the year in the same area was not recovered successfully and is believed to have been lost because of commercial fishing.) However, the study retains its importance since these data are the first current-meter data obtained from the inner and mid-shelf regions

of the West Florida Shelf, which is one of the widest and longest shelves off the United States.

Hourly sea-level heights were obtained at Cedar Key (see Fig. 1). A typical March reference level (104 cm) was used (Cragg *et al.*, 1982) which together with the linear trend implicitly removes the annual cycle from our sea-level data. The data were also adjusted for the inverted barometer effect using daily atmospheric pressure readings at Tampa. The sea-level series was filtered using the same filter as for the current-meter records. The synoptic variability is shown in Fig. 2.

Coastal winds were available at Tampa and at Apalachicola (Fig. 1). Cragg *et al.* (1982) showed that these two stations are within the coherence length of the wind field (their Fig. 4). For synoptic-band variability there is about a 6 h phase lag (Apalachicola leading) which is consistent with the fact that during this time of year the weather systems move through this area from NW to SE. Some data are available from an automatic recording station (DARDC Network) at Cedar Key but these data proved to be of little use owing to apparent large direction errors. To obtain a time series of winds on the shelf the records

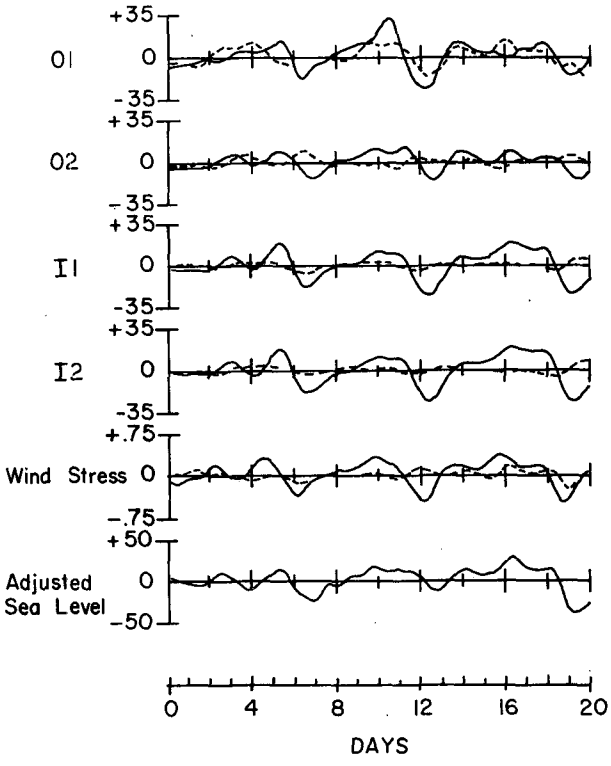

FIG. 2. Plot of the low-passed currents, wind stress and adjusted sea level. Solid line is the alongshore component and dotted one is the cross-shelf component. Filter used had 50% power point at 38 hours, <5% at 24 hours and >95% at 3.5 days. Units are cgs throughout and Day 0 corresponds to 1000 2/26/78. Depths of current meters were I1, 2: 12 m, 17 m; O1, 2: 9 m, 39 m, in depths of 22 and 44 m, respectively.

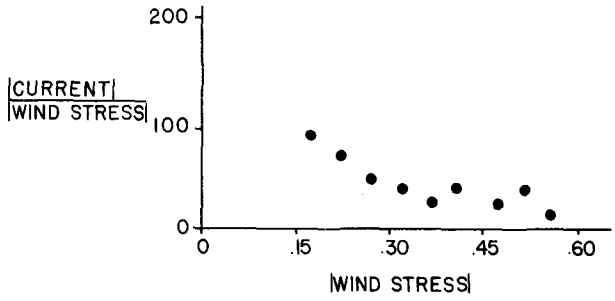

FIG. 3. Plot of the ratio of current speed (meter O1) to wind-stress magnitude (cm^{-1} s) as a function of wind-stress magnitude ($cm^2\ s^{-2}$) for stress exceeding 0.15 dyn cm^{-2}. Each point represents the average of all points falling in "bins" of stress magnitude 0.05 units wide. For example, the first point corresponds to the average of all the calculated ratios with wind stress between 0.15 and 0.20 dyn cm^{-2}.

at Tampa and Apalachicola were averaged after lagging Tampa and advancing Apalachicola by 3 h each to remove the phase difference between the two stations. This averaging may have underestimated the amplitude in the synoptic band because the Tampa and Apalachicola records were aligned only in an "average" sense. This also may have introduced phase uncertainties of several hours or more for individual wind events in the synoptic band. However, because all three series (Tampa, Apalachicola and their average) are similar, we do not expect the results to be sensitive to this averaging. Wind stress was calculated using a drag coefficient which varied linearly with wind speed (Wu, 1980), i.e., $C_D = (0.8 + 0.065\ W) \times 10^{-3}$ where W is the wind speed (m s^{-1}). The resulting series was filtered as the current records and sea-level heights were (Fig. 2).

3. Analysis and results

Fig. 2 shows a general picture of the synoptic-scale variability in the nearshore currents. The alongshore component of wind stress, adjusted sea level and the alongshore currents are all strikingly similar with sea level and currents lagging the stress by about half a day. At the inshore array (I1 and I2) the currents are barotropic to good approximation. Offshore (O1 and O2) there is definite vertical shear but both meters respond to the wind events nearly simultaneously. Similar results have been noted by others (e.g., Huyer *et al.*, 1978; Han and Mayer, 1981). Also, we note that there is no clear effect of cross-shelf wind stress on the currents or sea level and that the cross-shelf currents are generally smaller than 5 cm s^{-1}, except at the upper offshore meter. At these meters there is indication of return flow at depth in the cross-shelf velocity component, as noted elsewhere (Huyer, 1976). This is seen in the fact that the product of the cross-shelf components (not shown) is negative in five

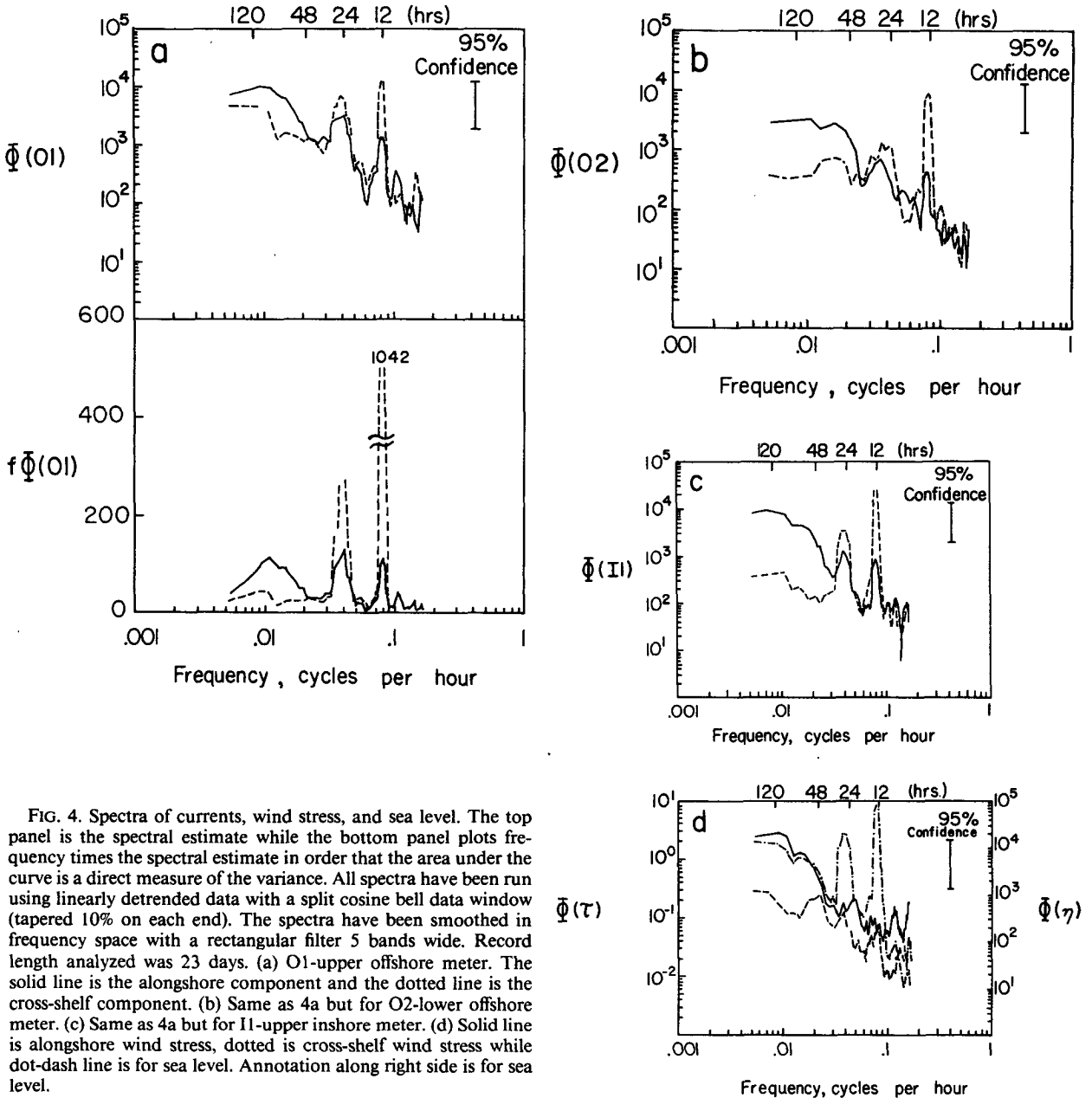

FIG. 4. Spectra of currents, wind stress, and sea level. The top panel is the spectral estimate while the bottom panel plots frequency times the spectral estimate in order that the area under the curve is a direct measure of the variance. All spectra have been run using linearly detrended data with a split cosine bell data window (tapered 10% on each end). The spectra have been smoothed in frequency space with a rectangular filter 5 bands wide. Record length analyzed was 23 days. (a) O1-upper offshore meter. The solid line is the alongshore component and the dotted line is the cross-shelf component. (b) Same as 4a but for O2-lower offshore meter. (c) Same as 4a but for I1-upper inshore meter. (d) Solid line is alongshore wind stress, dotted is cross-shelf wind stress while dot-dash line is for sea level. Annotation along right side is for sea level.

of six "events" when this product is significantly greater than zero. As is well known, we must be careful interpreting cross-shelf currents, because the cross-shelf component is much smaller than the alongshore one. Curvature of the isobaths makes the choice of the appropriate coordinate difficult.

Spectra of the records are shown in Fig. 4. The spectrum from I2 (not shown) is nearly identical to I1. About 70–90% of the variance appears to be in tides or in the synoptic band (Table 2). We also confirm a previous study in this area (Koblinsky, 1979) in finding that the semi-diurnal components (M_2 and S_2) are strongly cross-shelf and the diurnal ones (O_1 and K_1) also are but not so clearly. On the other hand, the synoptic variability is primarily in the alongshore component.

This partitioning of the variance is fortunate, as tides can be considered "noise" for a synoptic-band study. The similarity of I1 and I2 is expected from looking at Fig. 2. At the offshore array we again see indications of slightly different dynamics at the upper meter (O1) in that a significant portion (21.9%) of the synoptic variance is associated with the cross-shelf component. This is seen to a lesser degree at the lower

TABLE 3. Amplitudes of the four dominant tidal components. The record lengths used were 360 hours and 336 hours for M_2 and S_2, and O_1 and K_1, respectively. Two Fourier analyses were done; for the first and the last 336 (or 360) hours of the entire record. The data are hourly and are described in Table 2. The amplitude given is the average of the two runs, while the number in parentheses is half the difference between the two runs. Amplitudes are in cm s^{-1} for current meters and cm for sea level.

	M_2	S_2	O_1	K_1
V-O1	4.06 (1.10)	1.73 (0.63)	5.11 (1.24)	4.35 (0.03)
U-O1	13.81 (0.03)	6.18 (1.13)	7.29 (2.11)	5.57 (1.31)
V-O2	2.47 (0.43)	0.73 (0.17)	1.71 (0.73)	1.19 (0.61)
U-O2	11.47 (0.95)	5.55 (0.53)	3.25 (0.33)	1.94 (1.28)
V-I1	2.52 (0.47)	1.79 (0.66)	2.66 (1.26)	2.99 (1.21)
U-I1	19.12 (0.57)	9.35 (1.14)	5.19 (0.66)	4.91 (0.85)
V-I2	3.80 (0.11)	2.12 (0.55)	2.23 (1.70)	2.79 (1.31)
U-I2	18.45 (0.34)	9.29 (1.16)	5.01 (0.55)	4.60 (0.93)
Sea level	34.4 (0.3)	16.1 (2.4)	13.1 (0.6)	11.3 (2.4)

meter and is in contrast to the more strongly alongshore variability at the inshore array.

a. Tidal amplitudes

Although this experiment was not designed to study tides (the record length is 23 days), we present here an estimate of the amplitudes of the four dominant tidal components. To analyze for the components it was necessary to resolve them by choosing differing record lengths for analysis. Our choice (see Table 3) puts M_2 and S_2 near the center of adjacent frequency bands and thus simultaneously resolves them and prevents large amounts of leakage. This is true for O_1 and K_1 as well. Since our record length was slightly less than twice 360 hours, we were able to obtain two nearly independent estimates of the

TABLE 4. Results of cross-spectral analyses in the spectral band (2 to 20 days). For the cross-spectra run against either stress component 3 h current components or sea level were used. The original records were filtered with a Gaussian filter of standard deviation 6 h and subsampled at 3 h intervals. For the sea level-currents cross-spectra, hourly data (described in Table 2) were used. The spectra were recolored for the effects of the filters. The first of the two columns for the coherence, phase and response function is from a 3-band rectangular spectral filter (6 degrees of freedom) while the second is for a similar 5-band filter (10 degrees of freedom). These are averages over the band weighted by the square root of the cross-spectrum (the coherent amplitude). The numbers in parentheses are one standard deviation of the weighted mean. The phases are positive if stress lags currents or sea level, or if currents lag sea level. The response function is the ratio of the currents or sea level to stress or of sea level to currents. All units are cgs except the phase which is in hours.

	Coherence significance level		Average phase		Response function	
τ^y vs τ^x	53	68	−8 (11)	−8 (13)	0.24 (0.27)	0.21 (0.28)
η	96	100	−14 (1.7)	−13.3 (2.3)	59 (10)	57 (7)
V-O1	90	99	−9.3 (3.9)	−8.2 (1.9)	49 (16)	49 (18)
V-O2	98	100	−16.5 (4.4)	−15.4 (2.9)	35 (7)	34 (9)
V-I1	99	100	−13 (3)	−12 (2.6)	53 (6)	52 (6)
V-I2	98	100	−14 (3)	−13 (3)	55 (8)	54 (7)
U-O1	89	98	−9.2 (6.1)	−7.2 (2.4)	32 (9)	30 (10)
U-O2	78	92	−21 (76)	7.5 (79)	13 (8)	13 (9)
U-I1	80	94	5.6 (9)	6.7 (2.5)	8.7 (4.3)	8.5 (3.2)
U-I2	75	92	20 (37)	13 (11)	8 (3)	7.6 (2.5)
τ^x vs η	81	94	−4 (5.6)	−3.9 (5.9)	150 (53)	137 (60)
V-O1	16	21	−8 (22)	−11 (29)	60 (54)	44 (50)
V-O2	48	61	−9 (26)	−7 (14)	53 (30)	48 (38)
V-I1	46	61	−8 (16)	−6 (14)	85 (43)	77 (47)
V-I2	51	65	−9 (16)	−7 (14)	95 (51)	84 (52)
U-O1	48	55	−3 (33)	1 (32)	54 (31)	42 (32)
U-O2	54	64	046 (59)	−35 (61)	25 (13)	20 (16)
U-I1	29	35	9 (53)	23 (46)	14 (16)	12 (12)
U-I2	53	65	40 (48)	30 (34)	20 (14)	17 (12)
η vs V-O1	67	86	−5.9 (3)	−5 (4)	0.81 (0.26)	0.71 (0.21)
V-O2	92	99	1.6 (3.3)	1.7 (4.5)	1.61 (0.43)	1.52 (0.40)
V-I1	93	99	0.3 (5.1)	−0.6 (2.5)	1.04 (0.12)	1 (0.12)
V-I2	94	100	1.3 (5.6)	0.3 (2.8)	1.01 (0.12)	0.98 (0.09)
U-O1	78	92	−4.1 (6.2)	−5.3 (3.9)	1.33 (0.44)	1.21 (0.35)
U-O2	78	92	46 (41)	36 (31)	3.4 (1.6)	2.9 (1.9)
U-I1	69	85	−29 (39)	−23 (10)	3.6 (1.5)	3.4 (1.1)
U-I2	82	94	−40 (37)	−31 (20)	4.8 (1)	4.3 (0.5)

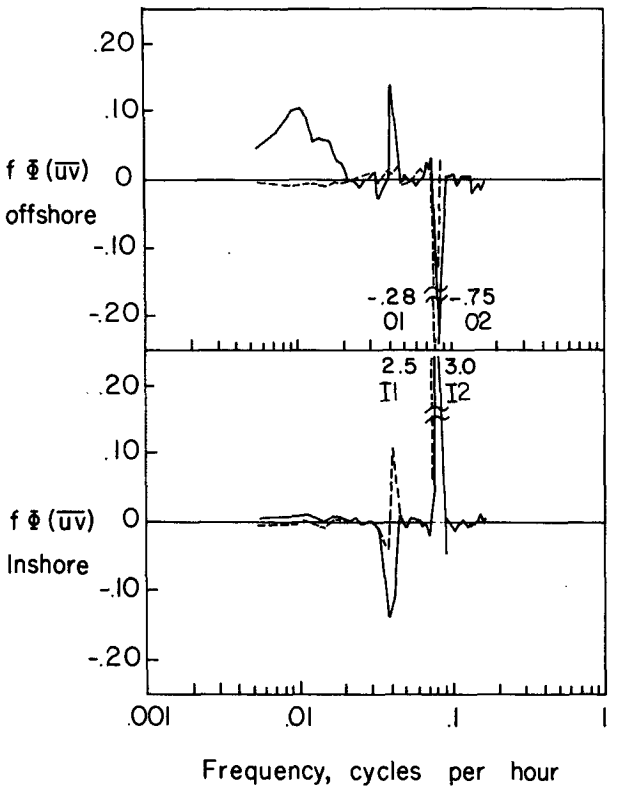

FIG. 5. Variance preserving frequency spectrum of $\overline{uv}$. Frequency times the spectral estimate is plotted so that the area under any portion of the curve is a direct measure of the contribution to the total $\overline{uv}$ of motions characterized by frequencies at that part of the curve. The solid line is for the upper meter and the dotted one is for the lower meter. Where the peaks go off scale the values at the extrema are given along with the associated current-meter label.

amplitudes. Table 3 shows the extent to which the tides are predominantly in the cross-shelf component. By comparing Table 3 and Figure 2, the tidal velocity in this area is seen to be about 15% larger than the synoptic motions.

The cross-shelf component of M_2 at O2 leads O1 by 26 min while that at I2 leads I1 by 7 min. Presumably this phase advance with depth is caused by bottom friction (e.g., Weisburg and Sturges, 1976). These amplitude and phase results are in excellent agreement with the analytic theory of Battisti and Clarke (1982).

b. *Wind forcing*

The cross-spectra between wind stress, current and adjusted sea-level heights are summarized in Table 4. The coherence is significant for all cross spectra using the alongshore component of wind; this result is true even for the cross-shelf components of the currents although it is not as striking and may be due to the contamination of the cross-shelf component by the alongshore current discussed earlier. Little coherence is seen with the cross-shelf wind stress. Apparently, for the magnitude of wind stress observed (order of 0.5 dyn cm^{-2}), the alongshore wind stress is the dynamically important forcing. Table 3 also shows that sea level and alongshore currents lag the alongshore stress by approximately half a day.

From the averaged response function it is clear that the cross-shelf component of O1 (upper offshore meter) responds more effectively to the alongshore forcing than that of O2 and much more so than the cross-shelf components of the inshore meters.

c. *uv correlations*

Fig. 5 shows the frequency structure of the Reynolds-stress term $\overline{uv}$ at each of the current meters. The tidal *uv*-products do correlate in this coordinate system but our main interest lies in the synoptic band. The plots are made in the same manner as a variance preserving plot for variance. The largest value is at O1 owing to its larger cross-shelf component. This result can be obtained, of course, in another fashion; cross-spectra of the cross-shelf and alongshore components show them to be nearly in phase at O1 but nearly out of phase at the inshore array.

Fig. 6 shows a plot of the *uv*-product versus time using the detrended, low-passed (synoptic band) data. It appears that at the upper offshore meter "pulses" of correlation may be associated with alongshore stress events. We interpret this result to imply that Ekman dynamics are more important at the offshore array than at the inshore one. From these calculations we estimate the magnitude of the upper-layer $\overline{uv}$ cross-shelf gradient as being on the order of 10^{-5} cm^2 s^{-2} between the two moorings. This gradient certainly may be important for studies on the shelf dealing with time scales significantly longer than the synoptic.

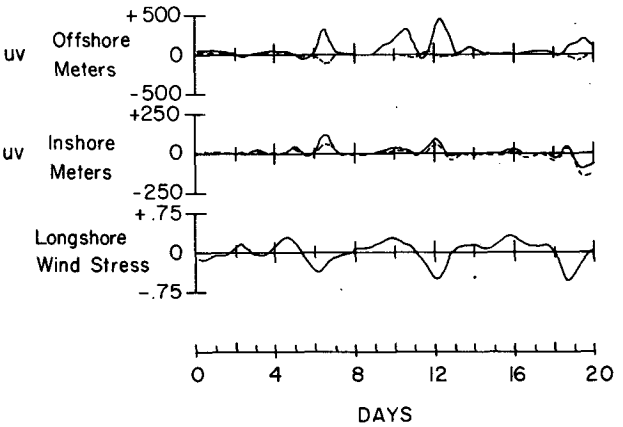

FIG. 6. Plot of the product of alongshore and cross-shelf velocities versus time. Day 0 corresponds to 1000 2/26/78 and the solid line is for the upper meter while the dotted one is for the lower meter.

d. Cross-shelf geostrophic length scale

If we integrate in the cross-shelf direction an assumed geostrophic balance in the x-momentum equation we obtain

$$L_g = \frac{g}{f}\frac{\Delta\eta}{\langle v\rangle}, \tag{1}$$

where L_g is the length scale, g the acceleration of gravity, f the Coriolis parameter, $\Delta\eta$ the sea level response and $\langle v\rangle$ the cross-shelf average surface current. We used the average of the alongshore components of O1 and I1 to approximate $\langle v\rangle$ and calculated the average of the term on the right-hand side of (1) for the duration of the data shown in Fig. 2 to estimate L_g. A second estimate was made by simply using the ratio of the amplitudes of individual events in the sea-level and current records. Both approaches yielded the result of 170 km for this length scale. This number is very close to the distance to the shelf break (200 km).

e. Linear friction parameter r

An early determination of an r-value was made off Long Island by Scott and Csanady (1976). They assumed a steady-state balance of alongshore wind and bottom stress and a steady alongshore pressure gradient in the depth-averaged y momentum equation where bottom stress is parameterized as rv_b and v_b is the near-bottom velocity. Since our inshore currents seem strongly barotropic, we replace v_b by simply the alongshore current v. Thus the equation becomes

$$\tau^y = rv + gh\frac{\partial\bar{\xi}}{\partial y}, \tag{2}$$

where τ^y is the alongshore stress, h the water depth and $\partial\bar{\xi}/\partial y$ the steady alongshore sea-level slope. Some objections have been raised to this procedure; these will be discussed more fully in the next section. Assuming this balance and using the method of batch averaging, which is discussed by Scott and Csanady (1976), we find $r = 0.018 \pm 0.001$ cm s^{-1} and a surface slope of $(0.6 \pm 1.0) \times 10^{-7}$ (Fig. 7). The remarkable linearity of this fit argues convincingly for the usefulness of the linear bottom-stress parameterization. The average alongshore slope is not significantly different from zero. This result is consistent with the previous finding (Cragg *et al.*, 1982) that the set-up on this shelf is symmetric with respect to alongshore stress of either sign.

The r value may also be obtained in a more straightforward fashion from the response function between alongshore stress and alongshore current at the inshore meters (Table 4). Since the coherence is significant at nearly the 100% level, the response function can be interpreted as an "in-phase" linear regression coefficient between the two series. At the upper meter (I1) this value of r is 0.019 ± 0.004 cm s^{-1} while at the lower meter (I2) r is 0.0185 ± 0.004 cm s^{-1}. The uncertainties are 2 standard deviations.

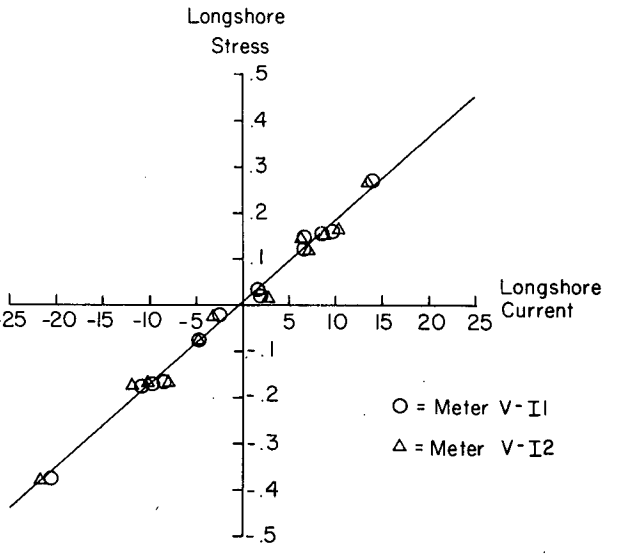

FIG. 7. Plot of alongshore stress versus alongshore current at the inshore array. Points represent "batch averaging" as by Scott and Csanady (1976) at both the upper meter (circles) and the lower meter (triangles) separately. The best-fit line to all the points is shown and is given by longshore stress = (0.018 ± 0.001) alongshore current + (0.6 ± 1.0). The uncertainties are ±2 standard deviations and represent approximate 95% confidence limits.

From an earlier paper (Csanady, 1978), the cross-shelf frictional scale can be calculated as

$$L_f = (2r/fks)^{1/2}, \tag{3}$$

where L_f is the frictional scale, r the friction parameter, f the Coriolis parameter, k the alongshore wavenumber of the forcing and s a linear estimate of bottom slope. One problem arises, however. For this scaling to be accurate we must use an "r" appropriate for the actual magnitude of the forcing, which is approximately twice as large out over the water as that measured at the coastal stations. Thus, using $r = 0.04$ cm s^{-1}, $s = 5 \times 10^{-4}$, $k = 2 \times 10^{-3}$ km^{-1}, we obtain the estimate of 100 km as the cross-shelf frictional length scale.

4. Discussion

As mentioned earlier, objections have been raised concerning the use of (2) in calculating an r-value. Specifically, Beardsley and Winant (1979) point out that the value of r thus calculated may be too large, since part of the alongshore wind stress may be balanced by synoptic-scale variations in the Coriolis term, fu, and the alongshore pressure gradient, rather than bottom stress alone. A recent numerical model

(Beardsley and Haidvogel, 1981) of the same area studied by Scott and Csanady (1976) suggest that as much as 50% of the wind stress may be balanced by these terms. Thus, the r value we calculated using (2) may be too large by as much as a factor of 2. Using this percentage, revised estimates of r for this study are 0.01–0.02 cm s^{-1} using coastal wind data or 0.02–0.04 cm s^{-1} when the increased wind stress over the water is taken into account. Similarly, the frictional length scale L_f is estimated to be 75–100 km.

The r-value on this shelf is rather small compared to a number of values given by Winant and Beardsley (1979). This is not surprising, however, in light of the relatively modest tidal currents in the study area. The friction parameter may be estimated as a drag coefficient times an rms tidal current (Csanady, 1976). Using 25 cm s^{-1} as a tidal rms value (Table 3) and a drag coefficient of $1–2 \times 10^{-3}$, r is estimated as 0.025–0.05 cm s^{-1}; this calculation is in good agreement with the above estimate.

5. Conclusion

The inshore array is within the frictional length scale and, since we find no evidence for a significant steady alongshore slope, the dominant alongshore momentum balance appears to be a simple balance between wind stress and bottom stress. The bottom stress is well parameterized as being linear in the barotropic alongshore current with a friction parameter of 0.01–0.02 cm s^{-1} if wind stress is calculated from coastal winds. In the cross-shelf equation, the data are consistent with an assumed geostrophic balance with a length scale roughly equal to the shelf width.

At the offshore array we did not calculate an r-value because the depth-averaged equations are inappropriate there on account of significant vertical shear. Also there appears to be an upper Ekman layer and an extended lower layer, in contrast to the barotropic response at the inshore array. This can also be seen in the fact that although O1 still responds primarily to alongshore wind stress, it has a significant cross-shelf component which leads to a positive $\overline{uv}$. We note that the calculated frictional length scale does indeed fall between these two arrays and apparently marks the change in the appropriate dynamics.

Acknowledgments. This work was supported by the State of Florida. Ship time on the R.V. *Bellows* was provided by the State University System of Florida. We especially thank Capts. G. Olson and B. Millander for skillful ship handling and enthusiastic support. Many colleagues helped in the field work, including Prof. G. L. Weatherly; we especially thank D. Szabo and J. Tamul. Tidal data were supplied by the U.S. National Ocean Survey; meteorological data from the National Climatic Center. We thank Ms. Patricia Arnold for valuable assistance with the manuscript.

REFERENCES

Allen, J. S., and P. K. Kundu, 1978: On the momentum, vorticity and mass balance on the Oregon shelf. *J. Phys. Oceanogr.*, **8,** 13–27.

Battisti, D. S., and A. J. Clarke, 1982: Estimation of near shore tidal currents on non-smooth continental shelves. *J. Geophys. Res.* (in press).

Beardsley, R. C., W. Boicourt, L. C. Huff and J. Scott, 1977: CMICE 76: A current meter intercomparison experiment conducted off Long Island in February-March 1976. WHOI Tech. Rep. 77-62. Woods Hole Oceanographic Institution, 123 pp.

——, and D. B. Haidvogel, 1981: Model studies of the wind-driven transient circulation in the Middle Atlantic Bight. Part 1: Adiabatic boundary conditions. *J. Phys. Oceanogr.*, **11,** 355–375.

——, and C. D. Winant, 1979: On the mean circulation in the Mid-Atlantic Bight. *J. Phys. Oceanogr.*, **9,** 612–619.

Chesser, S. A., 1974: Sediments of the West Florida Shelf. M.S. thesis, Florida State University, Department of Oceanography, 71 pp.

Cragg, J., G. T. Mitchum and W. Sturges, 1982: Wind-induced sea-surface slopes on the West Florida Shelf. Submitted to *J. Phys. Oceanogr.*

——, and W. Sturges, 1974: Wind-induced currents and sea-surface slopes in the Eastern Gulf of Mexico. M.S. thesis, Florida State University, Department of Oceanography, 51 pp.

Csanady, G. T., 1976: Mean circulation in shallow seas. *J. Geophys. Res.*, **81,** 5389–5399.

——, 1978: The arrested topographic wave. *J. Phys. Oceanogr.*, **8,** 47–62.

Han, G. C., and D. Mayer, 1981: Current structure on the Long Island Inner Shelf. *J. Geophys. Res.*, **86,** 4205–4214.

Huyer, A., 1976: A comparison of upwelling events in two locations: Oregon and Northwest Africa. *J. Mar. Res.*, **34,** 531–546.

——, R. L. Smith and E. J. C. Sobey, 1978: Seasonal differences in low-frequency current fluctuations over the Oregon Continental Shelf. *J. Geophys. Res.*, **83,** 5077–5089.

Koblinsky, C. J., 1979: Tides on the West Florida Shelf. Ph.D. thesis. Oregon State University, 110 pp.

——, and P. P. Niiler, 1980: Direct measurements of circulation on West Florida Continental Shelf January 1973–May 1975. Data Report 76. Reference 79-13. School of Oceanography/Oregon State University, 102 pp.

Niiler, P. P., 1976: Observations of low-frequency currents on the West Florida Continental Shelf. *Mem. Soc. Roy. Sci. Liege,* **6,** 331–358.

Pettigrew, N. R., 1981: The dynamics and kinematics of the coastal boundary layer off Long Island. Ph.D. thesis, Massachusetts Institute of Technology/Woods Hole Oceanographic Institution WHOI-81-14.

Scott, J. T., and G. T. Csanady, 1976: Nearshore currents off Long Island. *J. Geophys. Res.*, **81,** 5401–5409.

SUSIO, 1975: Compilation and summation of historical and existing physical oceanographic data from the eastern Gulf of Mexico. Report to Bureau of Land Management—Contract 08550-CT4-16, 97 pp.

Weisburg, R. H., and W. Sturges, 1976: Velocity observations in the west passage of Narragansett Bay: A partially mixed estuary. *J. Phys. Oceanogr.*, **6,** 345–354.

Winant, C. D., and R. C. Beardsley, 1979: A comparison of some shallow wind-driven currents. *J. Phys. Oceanogr.*, **9,** 218–220.

Wu, J., 1980: Wind-stress coefficients over sea surface near neutral conditions—A revisit. *J. Phys. Oceanogr.*, **10,** 727–740.